# Polarization Vortices in Germanium Telluride Nanoplatelets: A Theoretical Study

E. Durgun,[1,2] Ph. Ghosez,[1,2] R. Shaltaf,[3,4,*] X. Gonze,[3,4] and J.-Y. Raty[1,2]

[1]*Physique Theorique des Matériaux, Université de Liège (B5), B-4000 Liège, Belgium*
[2]*European Multifunctional Materials Institute (EMMI), B-4000 Liège, Belgium*
[3]*Unité P.C.P.M., Université Catholique de Louvain, B-1348 Louvain-la-Neuve, Belgium*
[4]*European Theoretical Spectroscopy Facility (ETSF), B-1348 Louvain-la-Neuve, Belgium*

(Received 26 June 2009; published 7 December 2009)

Using first-principles calculations based on density functional theory, we study the properties of germanium telluride crystalline nanoplatelets and nanoparticles. Above a diameter of 2.7 nm, we predict the appearance of polarization vortices giving rise to an unusual ferrotoroidic ground state with a spontaneous and reversible toroidal moment of polarization. We highlight the crucial role of inhomogeneous strain in stabilizing polarization vortices. Combined with the phase-change properties of germanium telluride, the ferrotoroidic properties could be of practical interest for ternary logic applications.

DOI: 10.1103/PhysRevLett.103.247601 PACS numbers: 77.80.Bh, 61.46.−w, 77.84.−s, 85.50.Gk

Germanium telluride, GeTe, is well known for its phase-change properties [1]. The possibility to switch, by an intense laser pulse or Joule heating, between a metastable crystalline phase and an amorphous state which can be differentiated by large electrical and optical contrasts makes it extremely promising in view of memory applications [1–3]. Independently, and though it has been marginally discussed, GeTe is also a prototypical ferroelectric crystal with a spontaneous polarization, $P \approx 60\ \mu\mathrm{C/cm^2}$ and a Curie temperature, $T_c \approx 720$ K [4,5]. In principle, its switchable spontaneous polarization offers an alternative possibility for data-storage applications but this is not practically exploited at the bulk level because of a too low resistivity due to a high concentration in intrinsic vacancies [6].

Recently, GeTe nanowires have been synthesized [7,8], and a structural phase transition has been reported for diameters ranging from 20 to 200 nm and lengths up to $\sim 50\ \mu$m [9]. At this stage, however, very little attention has been paid to the evolution of the ferroelectric properties in GeTe nanostructures, although ferroelectricity is well known to be strongly influenced by finite size effects [10,11]. In ferroelectric oxides, it is now well understood that ferroelectricity is strongly dependent of electrical and mechanical boundary conditions [11,12]. In thin films, it was demonstrated that in the absence of screening, the depolarizing field arising from the uncompensated polarization charges at the surface forbid the appearance of any net polarization below a critical thickness, and so suppresses the ferroelectric phase transition [13]. In isolated zero and one-dimensional structures such as nanodots, nanodisks, and nanorods, depolarizing issues also forbids the appearance of a ferroelectric ground state but it was shown using theoretical arguments, that an alternative type of phase transition may exist [14]. Using an effective Hamiltonian parameters' fitting to first-principles calculations of bulk crystals, Naumov and collaborators have first shown that the ground-state structure of $BaTiO_3$ and $Pb(Zr, Ti)O_3$ dots and wires is a distorted cubic structure in which local dipoles are arranged in an unexpected vortex pattern [15,16]. This pattern does not induce any net macroscopic polarization ($\mathbf{P} = N^{-1}\sum_i \mathbf{p}_i = 0$, where $\mathbf{p}_i$ is the local dipole of cell $i$ located at $\mathbf{R}_i$, and $N$ is the number of cells in the structure) but produces a toroidal moment of polarization defined as $\mathbf{G} = \frac{1}{2N}\sum_i \mathbf{R}_i \times p_i$. The orientation of $\mathbf{G}$ can be either up or down depending whether the dipole moments rotate either clockwise or anticlockwise and an external control of $\mathbf{G}$ would open new opportunities for data-storage applications [15]. Different ways of switching $\mathbf{G}$ such as the use of transverse inhomogeneous electric fields [17] or a time-dependent magnetic field [15] have already been investigated at the theoretical level.

In this Letter, we demonstrate the existence of a spontaneous and switchable toroid moment of polarization in GeTe nanoparticles directly from fully atomistic first-principles calculations based on density functional theory. We discuss the evolution of the stability of polarization vortices with the size of the nanoparticle and highlight the existence of a critical radius for the appearance of a spontaneous $\mathbf{G}$. We also point out the key role of inhomogeneous strains in stabilizing the vortex pattern and discuss potential applications of our findings.

Our calculations were performed within density functional theory (DFT) [18], implemented in VASP package [19]. We used PAW potentials including Ge $4s^2 4p^2$ and Te $5s^2 5p^4$ electrons as valence states [20]. The exchange-correlation potential was approximated within the generalized gradient approximation [21]. We worked with periodic boundary conditions. In order to avoid interactions between periodic replica and access the properties of isolated platelets, we included a 10 Å vacuum region in all directions. The convergence of the results in terms of the vacuum region was double checked from comparison with independent calculations by using the ABINIT [22] package,

 

which allows for the nonperiodic simulation of isolated structures using a wavelets basis [23]. The Brillouin zone was sampled at the $\Gamma$ point only. We used a plane-wave basis set with a kinetic energy cutoff of 250 eV, which was checked to be sufficient to get fully converged results. The structure was relaxed using the conjugate gradient method with simultaneous minimization of the total energy and interatomic forces. The convergence on the energy was set to $10^{-6}$ eV, and the maximum residual force allowed on each atom was fixed at $10^{-3}$ eV/Å.

In what follows, we consider GeTe nanoplatelets which belong to a set of platelets similar to the one in Fig. 1(a) with generic formula $n \times n \times 2$, where $n$ corresponds to the number of atoms along $x$ and $y$ directions and ranges from 4 (32 atoms) to 18 (648 atoms). Starting from a truncated bulk cubic rocksalt structure, we then performed full atomic relaxation in order to determine their ground-state structure.

As a first step, we wanted to identify the highest-symmetry paraelectric (PE) reference structure. We so performed full atomic relaxation under $D_{2d}$ ($P$-42$m$) symmetry constraints, which forbid the appearance of any nonzero value of $\mathbf{P}$ or $\mathbf{G}$. For the $16 \times 16 \times 2$ platelet, we observed a global shrinking of the structure during the relaxation [Fig. 1(b)]. The bond lengths between nearest Ge and Te atoms ($d_{\text{Ge-Te}}$) in the core region of the relaxed structure range between 3.02 and 3.06 Å, which is similar to the paraelectric bulk-crystal value (3.01 Å). However, the distribution of bond lengths is not homogenous and $d_{\text{Ge-Te}}$ is shorter for edge and corner atoms. The thickness of the nanoplatelet is also smaller than the shortest bond length and is equal to ~2.7 Å due to surface relaxation effects. Looking at two consecutive planes along $z$, Ge (respectively Te) atoms move toward the interior (respectively exterior) of the cluster. Similar structural features are observed for the other platelet sizes. The evolution of the cohesive energy ($E_C$) is reported in Fig. 1(c). It progressively increases with the size of the system and tends gradually to the value observed for an infinite bilayer structure (6.32 eV/pair), itself slightly smaller than the paraelectric bulk-crystal value (6.40 eV/pair). We also further considered the possibility of $C_{2v}$ (Cmm2), and $D_2$ (P222) lower symmetry paraelectric structures but without any additional gain of energy, so confirming the $D_{2d}$ character of the PE reference.

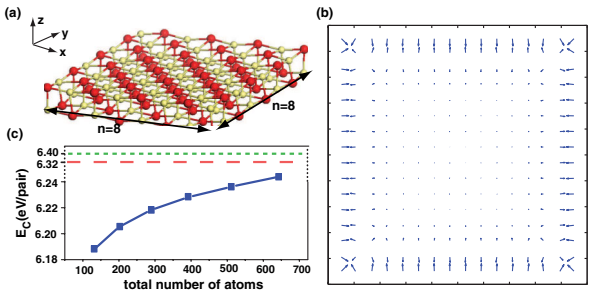


FIG. 1 (color online). (a) Atomic structure of a $n \times n \times 2$ GeTe nanoplatelet for $n = 8$. The structure consists in two consecutive atomic layers of Ge (dark balls) and Te (light balls) atoms along $z$ so that a Ge–Te pair can be affected to any given position $i$ in the $xy$ plane. (b) Top view of the relaxation pattern of a $16 \times 16 \times 2$ nanoplatelet with respect to initial bulk atomic positions, under the constraint of $D_{2d}$ symmetry. (c) Cohesive energy per Ge–Te pair, $E_C$, as a function of size for $n \times n \times 2$ nanoplatelets in the $D_{2d}$ symmetry. The dashed and dotted horizontal lines correspond to $E_C$ for a 2D infinite slab and for 3D crystal, respectively.

As a second step, we looked for possible structural distortion patterns able to further decrease the energy of the $D_{2d}$ paraelectric reference. To that end we performed new structural relaxations without imposing any symmetry constraint. For the $16 \times 16 \times 2$ platelet, we obtained a new ground-state structure with $S_4$ ($P$-4) symmetry, whose total energy is 740 meV (i.e., 2.89 meV per GeTe pair) below that of the PE reference.

In order to better characterize the type of atomic distortion which gave rise to this ground-state configuration, we computed the difference of atomic positions, $\Delta\mathbf{r}_i^{\text{Ge}}$ and $\Delta\mathbf{r}_i^{\text{Te}}$, between the ground state and the PE reference structures for each in-plane position $i$ [see Fig. 1] [24]. A top view of the results is illustrated in Fig. 2(a) and highlights the appearance of local dipoles $\mathbf{p}_i$, from unequal ionic displacements $\Delta\mathbf{r}_i^{\text{Ge}}$ and $\Delta\mathbf{r}_i^{\text{Te}}$. Coherently with the $S_4$ symmetry, the arrangement of dipoles is such that the macroscopic polarization $\mathbf{P}$ is exactly zero, which confirms the suppression of ferroelectricity due to depolarizing field issues in absence of screening. However, as can be anticipated from the arrangement of dipoles, there is a nonzero toroidal moment of polarization $\mathbf{G}$ oriented along $z$ [Fig. 1(a)]. Using the Born effective charges of the bulk cubic structure ($Z^* = 10.68$ e) [5] to compute the local dipoles, $\mathbf{p}_i = Z_i^{*\text{Ge}}\Delta\mathbf{r}_i^{\text{Ge}} + Z_i^{*\text{Te}}\Delta\mathbf{r}_i^{\text{Te}}$, we estimated the spontaneous $G$ of the ground-state structure to 14.4 eÅ$^2$ [25], a value comparable in amplitude to what was previously reported in the class of $ABO_3$ [15]. This confirms at the first-principles level that local polar distortions are not suppressed in isolated ferroelectric nanoparticles but are rearranged in an unusual vortex pattern to accommodate the electrical boundary conditions.

As might have been anticipated, starting from the paraelectric reference, the atomic distortions can be frozen in such a way that local dipoles rotate clockwise or anticlockwise, yielding two equivalent energy minima with a spontaneous macroscopic $\mathbf{G}$ or $-\mathbf{G}$ and a typical internal-energy double well [Fig. 3(b) inset] similar to that of usual ferroelectrics. However, since the order parameter is no more $\mathbf{P}$, such a system cannot strictly speaking be called ferroelectric and will rather be referred here to as ferrotoroidic (FT) with an order parameter $\mathbf{G}$.

The amplitude of the internal-energy double-well depth, $\Delta E_{\text{DW}}$, is significant but small for the $16 \times 16 \times 2$ nano-

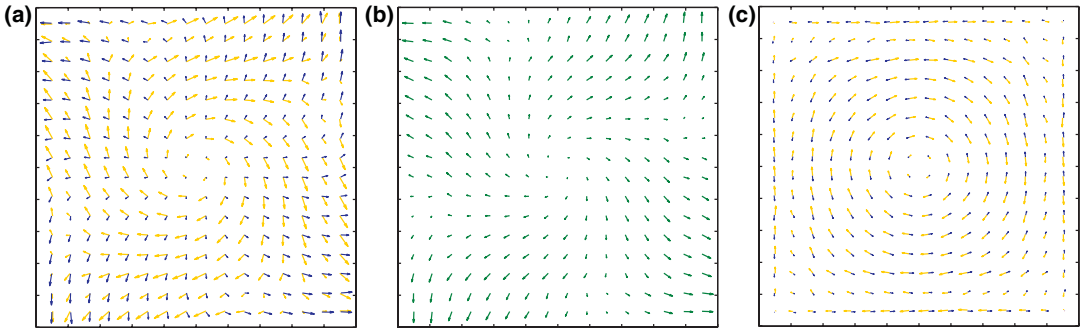


FIG. 2 (color online). Top view of (a) the individual ferrotoroidic polar distortions, $\Delta\mathbf{r}_i^{\mathrm{Ge}}$ (light arrows) and $\Delta\mathbf{r}_i^{\mathrm{Te}}$ (dark arrows), for the $16 \times 16 \times 2$ nanoplatelet. For the same nanoplatelet, decomposition of $\Delta\mathbf{r}_i^{\mathrm{Ge}}$ and $\Delta\mathbf{r}_i^{\mathrm{Te}}$ into (b) the displacement $\eta_i$ of the center of mass of each vertical Ge–Te pair and (c) the structural distortion $\xi_i^{\mathrm{Ge}}$ (light arrows) and $\xi_i^{\mathrm{Te}}$ (dark arrows).

platelet (2.89 meV per Ge–Te pair) so that we anticipate a low critical temperature $T_c$ for the FT phase transition. However, this critical temperature will increase with an increasing system size. The evolution of $\Delta E_{\mathrm{DW}}$ and $\mathbf{G}$ with the size of the platelet is summarized in Fig. 3, highlighting the existence of a critical size for the appearance of the FT distortion. Up to $n = 8$, the system remains paraelectric down to 0 K while at $n = 10$ it will start developing a nonzero $\mathbf{G}$ [26]. The amplitude of $\mathbf{G}$ then progressively increases with $n$ together with the double-well depth amplitude and the related value of $T_c$.

In Fig. 3(a), we also report in inset a top view of the local dipole pattern $\mathbf{p}_i$ for $n = 10$ and $n = 16$. The amplitude of the FT distortion is reduced in the center of the platelet and then increases with $\mathbf{R}$. In the subsurface layer however, in which the surface relaxation is large [Fig. 1(b)], the amplitude of the motion significantly decreases again. From Fig. 3, it appears that the FT distortion cancels out when the central and surface regions with reduced distortions start overlapping.

We did not only consider the square platelets, but rounder geometries in which 1 to 3 Ge–Te pairs at each corner have been removed as well. In these structures a similar vortex pattern is obtained with only a slight reduction in $E_C$ and $G$ as shown in Fig. 3(a). This indicates that the formation of vortex pattern is not particular to a specific shape.

We also looked at the evolution of $\mathbf{G}$ with the thickness $m$ of the platelets. The results are summarized in Fig. 3(c). They reveal that, contrary to what happens with the radius of the platelet, $\mathbf{G}$ very rapidly saturates to a constant value with thickness.

When building model Hamiltonians to study the behavior of ferroelectric nanodots, the main degree of freedom is typically the local polar distortion associated to the bulk ferroelectric soft mode. Looking at Fig. 2(a), we see here that Ge and Te atoms are displaced locally in nearly perpendicular directions, which contrasts with what would be expected from a simple condensation of the local distortion associated to the bulk ferroelectric soft mode. In order to clarify this behavior, we decomposed the distortion $\Delta\mathbf{r}_i^{\mathrm{Ge,Te}}$ of Ge and Te atoms at in-plane position $i$ in terms of the motion $\eta_i$ of the center of mass of the Ge-Te pair at site $i$ and of the additional polar motion $\xi_i^{\mathrm{Ge,Te}}$ of the atoms respect to the center of mass:

$$\Delta\mathbf{r}_i^{\mathrm{Ge,Te}} = \eta_i + \xi_i^{\mathrm{Ge,Te}}. \quad (1)$$

The results are illustrated in Figs. 2(b) and 2(c) for the $16 \times 16 \times 2$ nanoplatelet. The first contribution $\eta_i$ is a nonpolar distortion which can be interpreted as an inhomogeneous strain relaxation [27] and we checked for all sizes that the condensation of $\eta_i$ alone never decreases the energy, confirming the $D_{2d}$ character of the PE reference. The second contribution $\xi_i^{\mathrm{Ge,Te}}$ is the polar motion related to the bulk ferroelectric soft mode. It is the primary order

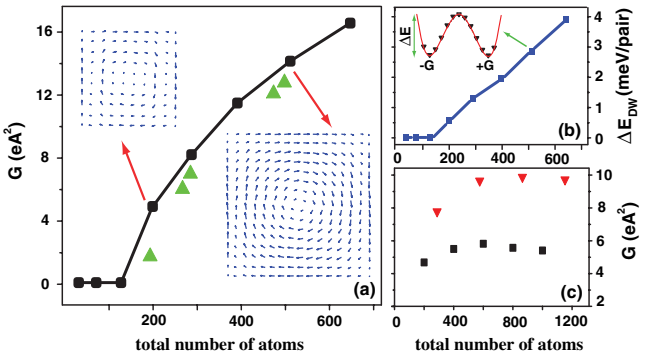


FIG. 3 (color online). (a) Evolution of the spontaneous toroidal moment of polarization, $\mathbf{G}$ (square data points) in terms of the number of atoms in $n \times n \times 2$ nanoplatelets. The values of $\mathbf{G}$ for platelets in which from 1 to 3 pairs of Ge–Te atoms are cut at each corner (rounder cross section) are also reported (triangular data points). A top view of the local dipole moments $\mathbf{p}_i$ (arrows) is shown in the inset for $n = 8$ and $n = 16$. (b) The variation of internal-energy double-well depth, $\Delta E_{\mathrm{DW}}$ in terms of the number of atoms in $n \times n \times 2$ nanoplatelets. The dependence of double-well on $\mathbf{G}$ for $16 \times 16 \times 2$ is given as the inset. (c) Evolution of $\mathbf{G}$ for $10 \times 10 \times m$ ($m = 2$ to 10) (square data points) and $12 \times 12 \times m$ ($m = 2$ to 8) (triangular data points) nanoparticles.

parameter of the FT phase transition but surprisingly, this single distortion only becomes unstable in $n \times n \times 2$ nanoplatelets for $n$ larger than 14 and, alone, yields a much weaker gain of energy than the one reported for the ground state. This points out the crucial role of the coupling of $\xi_i$ with the homogeneous strain relaxation $\eta_i$ in order to stabilize the FT ground state and importance of properly including both degrees of freedom in model Hamiltonians intended to describe the properties of GeTe nanoparticles. Interestingly, in the range $n = 10$–$14$, neither $\eta_i$ nor $\xi_i$ is individually unstable while it is only their coupling that is giving rise to the stabilization of the FT ground state. This suggests the existence of an unusual phase transition mechanism without any primary order parameter in the range of sizes and certainly motivates for further investigations.

We have demonstrated here the existence of a spontaneous and switchable toroidal moment of polarization **G** in the crystalline phase of GeTe nanoplatelets. Beyond the fundamental interest of exploring ferrotoroidal properties at the nanoscale, these results are also of direct interest for technological applications. The amplitude of **G** in GeTe is comparable to what was previously reported in the class of $ABO_3$ compounds, which enlarges the field of investigations for memory devices exploiting the toroidal moment of polarization to an alternative type of compounds, not considered before and more compatible with the semiconductor technology. Going further, GeTe is not only limited to the applications envisaged for $ABO_3$ compounds, as its phase-change ability combined with this switchable toroidal polarization also makes it an adequate candidate for a 3-states recording (two crystalline states with $+\mathbf{G}$ and $-\mathbf{G}$ and one amorphous state) at the nanoparticle level. The idea of ternary logic appeared together with ternary computers decades ago and is subject to a renewed of interest [28] due to its intrinsic superiority to binary logic. We hope that the unexpected combination of properties offered by GeTe nanoparticles that opens new perspectives for data-storage applications will stimulate further studies and experimental validation of our theoretical findings.

The authors thank E. Schwegler, M. Verstraete, and P. Dauby for fruitful discussions and acknowledge financial support from the Belgian FNRS and the Interuniversity Attraction Poles Program (Grant No. P6/42)-Belgian State-Belgian Science Policy. The calculations were performed with the support of the Lawrence Livermore National Laboratory and the TUBITAK-ULAKBIM High Performance Computing Center (Turkey).

*Present address: Department of Physics, University of Jordan, 11942, Amman, Jordan.

[1] J. Akola and R. O. Jones, Phys. Rev. B **76**, 235201 (2007).
[2] K. Shportko, S. Kremers, M. Woda, D. Lencer, J. Robertson, and M. Wuttig, Nature Mater. **7**, 653 (2008).
[3] W. Welnic, S. Botti, L. Reining, and M. Wuttig, Phys. Rev. Lett. **98**, 236403 (2007).
[4] K. M. Rabe and J. D. Joannopoulos, Phys. Rev. B **36**, 6631 (1987).
[5] R. Shaltaf, E. Durgun, J.-Y. Raty, Ph. Ghosez, and X. Gonze, Phys. Rev. B **78**, 205203 (2008).
[6] A. H. Edwards *et al.*, J. Phys. Condens. Matter **17**, L329 (2005).
[7] D. Yu, J. Q. Wu, Q. A. Gu, and H. K. Park, J. Am. Chem. Soc. **128**, 8148 (2006).
[8] X. Sun, B. Yu, G. Ng, and M. Meyyappan, J. Phys. Chem. C **111**, 2421 (2007).
[9] S-H. Lee, D-K. Ko, Y. Jung, and R. Agarwal, Appl. Phys. Lett. **89**, 223116 (2006).
[10] C. H. Ahn, K. M. Rabe, and J.-M. Triscone, Science **303**, 488 (2004).
[11] J. Junquera and Ph. Ghosez, J. Comput. Theor. Nanosci. **5**, 2071 (2008).
[12] K. M. Rabe, Curr. Opin. Solid State Mater. Sci. **9**, 122 (2005).
[13] J. Junquera and Ph. Ghosez, Nature (London) **422**, 506 (2003).
[14] I. Ponomareva, I. Naumov, I. Kornev, H. Fu, and L. Bellaiche, Curr. Opin. Solid State Mater. Sci. **9**, 114 (2005).
[15] I. Naumov, L. Bellaiche, and H. Fu, Nature (London) **432**, 737 (2004).
[16] H. Fu and L. Bellaiche, Phys. Rev. Lett. **91**, 257601 (2003).
[17] S. Prosandeev, I. Ponomareva, I. Kornev, I. Naumov, and L. Bellaiche, Phys. Rev. Lett. **96**, 237601 (2006).
[18] W. Kohn and L. J. Sham, Phys. Rev. **140**, A1133 (1965); P. Hohenberg and W. Kohn, Phys. Rev. **136**, B864 (1964).
[19] G. Kresse and J. Hafner, Phys. Rev. B **47**, 558 (1993); G. Kresse and J. Furthmuller, Phys. Rev. B **54**, 11 169 (1996).
[20] P. E. Blochl, Phys. Rev. B **50**, 17 953 (1994).
[21] J. P. Perdew *et al.*, Phys. Rev. B **46**, 6671 (1992).
[22] X. Gonze *et al.*, Comput. Mater. Sci. **25**, 478 (2002).
[23] L. Genovese *et al.*, J. Chem. Phys. **129**, 014109 (2008).
[24] To avoid arbitrary rigid translation and rotation of the cluster when comparing the atomic positions in the PE reference and ground-state structure, the position of the center of mass of the cluster was kept fixed and the principal inertia axis of the two structures were aligned.
[25] Although the conventional approach [15], assuming $Z^*$ constant typically yields an overestimate of $G$. In GeTe, from the strong dependency of $Z^*$ to atomic displacement [5], this overestimate can be estimated to $\approx 30\%$. This inaccuracy on the absolute value of $G$ does not affect the FT distortion pattern nor our main conclusions.
[26] This is what is expected in a classical framework, while zero-point quantum vibrations might influence the critical size. See, e.g., A. R. Akbarzadeh *et al.*, Phys. Rev. B **70**, 054103 (2004).
[27] S. Prosandeev, I. Kornev, and L. Bellaiche, Phys. Rev. B **76**, 012101 (2007).
[28] M. Klein, S. Rogge, F. Remacle, and R. D. Levine, Nano Lett. **7**, 2795 (2007).